

Appendices - Supplementary Information

Circular versus linear RNA topology: different modes of RNA-RNA interactions in vitro and in human cells.

Sonja Petkovic et al.

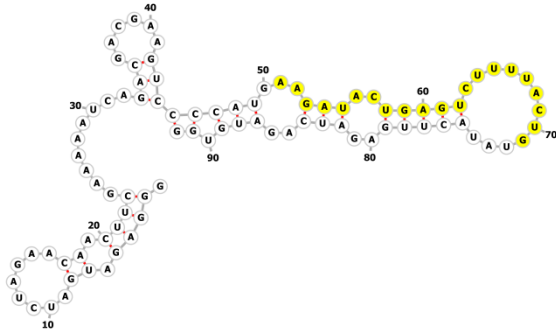
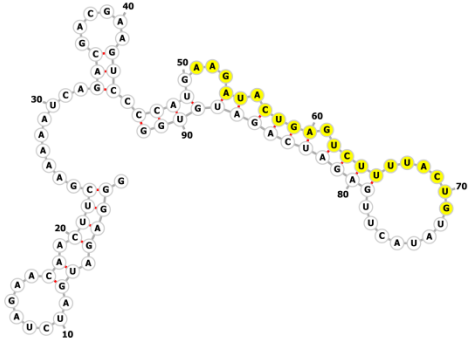
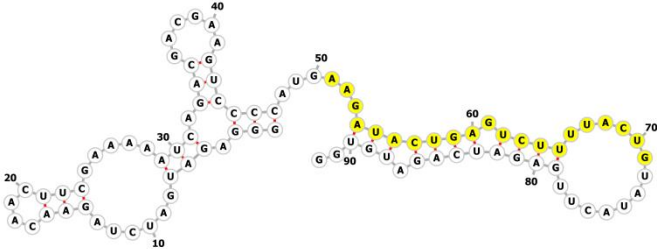
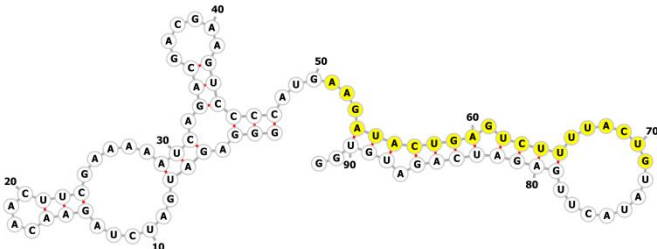
sonja.petkovic@neuro.uni-luebeck.de and georg.sczakiel@uni-luebeck.de

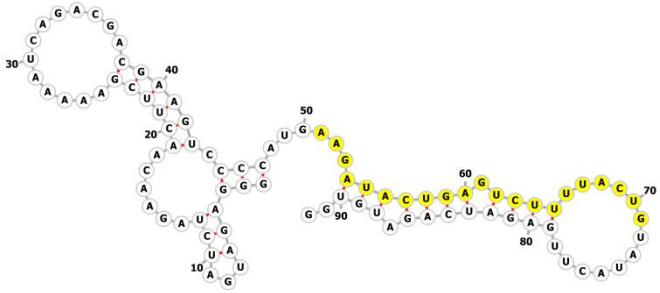
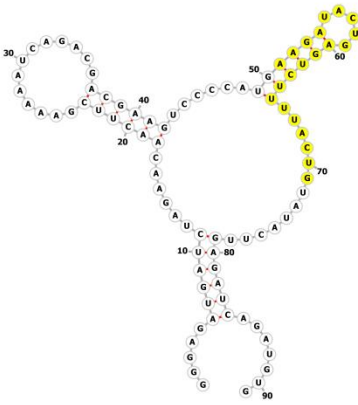
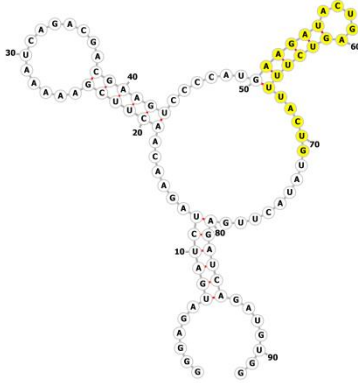
1. Supplementary Figures	2
Figure S1: Secondary structure predictions 92mers	2
Figure S2: Dependency of rate constants on RNA length and topology	26
Figure S3: Associative pathway vs. dissociative pathway	27
Figure S4: Intracellular amounts of lin-92 and circ-92, respectively after transfection	28
Figure S5: The order of the transfection of plasmids and RNAs does not influence the observations of competing lin-92/circ-92	29
2. Supplementary Tables	30
Table S1: RNA sequences (92mer - 182mer)	30
Table S2: Sequences of small antisense RNAs and miRNAs	31
Table S3: Primer sequences and sequence of stocking oligonucleotide	32
Table S4: Dependency of rate constants on RNA length and topology	33
Table S5: Thermodynamic parameters of the association of as101 and lin-92 and circ-92, respectively.	34

Figure S1 Temperature-dependency of secondary structure predictions of bladder cancer associated RNAs 92-182mer applying different temperatures and the software: RNAfold and forna (Nov 05, 2017) from ViennaRNA package 2.4.1

lin-92

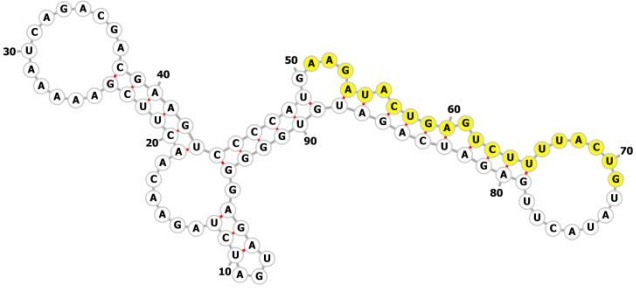
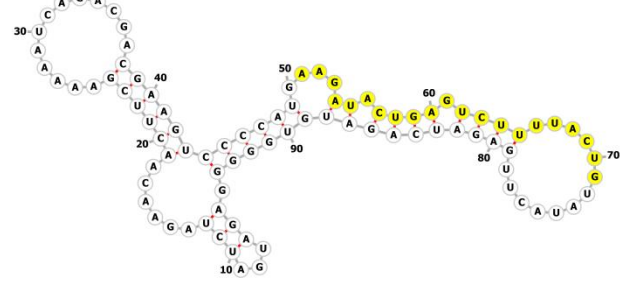
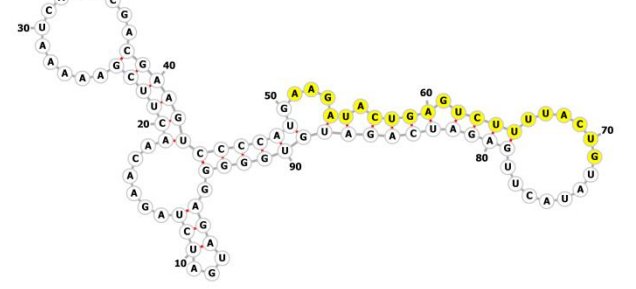
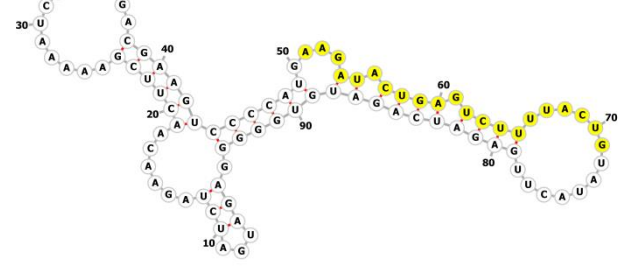
GGGAGAUGAUCUAGAACAACUUCGAAAAUCAGACGACGAAGUCCCAUGAAGAUACU
GAGUCUUUUACUGUAUACUUGAGAUCAGAUGUGG

Temperature [°C]	Secondary structure
13	
20	
25	
30	

<p>37</p>	 <p>Secondary structure diagram of an RNA sequence (37). The sequence is numbered from 1 to 90. A region from approximately position 50 to 75 is highlighted in yellow. The structure shows several stem-loops and a large internal loop.</p>
<p>45</p>	 <p>Secondary structure diagram of an RNA sequence (45). The sequence is numbered from 1 to 90. A region from approximately position 50 to 75 is highlighted in yellow. The structure is similar to sequence 37 but with a different internal loop configuration.</p>
<p>52</p>	 <p>Secondary structure diagram of an RNA sequence (52). The sequence is numbered from 1 to 90. A region from approximately position 50 to 75 is highlighted in yellow. The structure is very similar to sequence 45, showing a different internal loop configuration.</p>

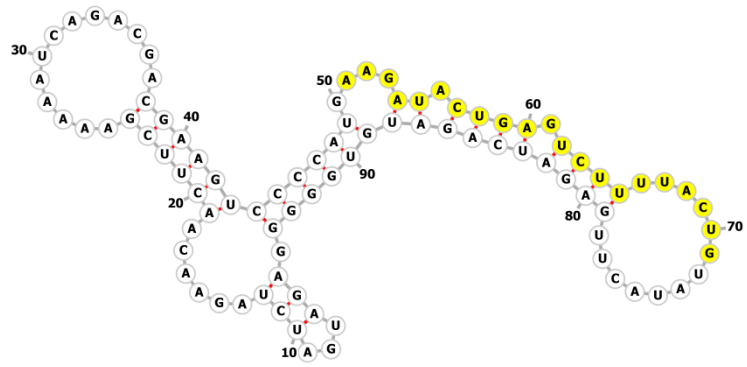
circ-92

GGGAGAUGAUCUAGAACAACUUCGAAAAUCAGACGACGAAGUCCCAUGAAGAUACU
 GAGUCUUUUACUGUAUACUUGAGAUCAGAUGUGG

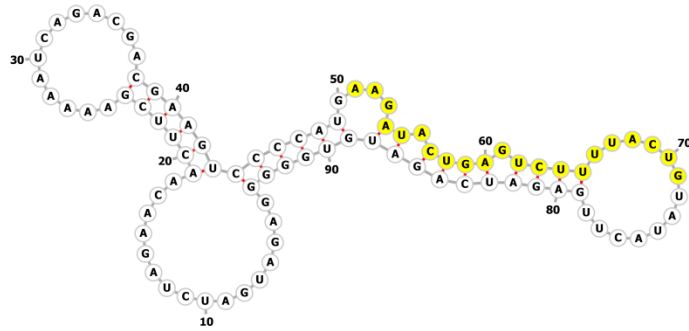
Temperature [°C]	Secondary structure
13	
20	
25	
30	

(continued
circ-92)

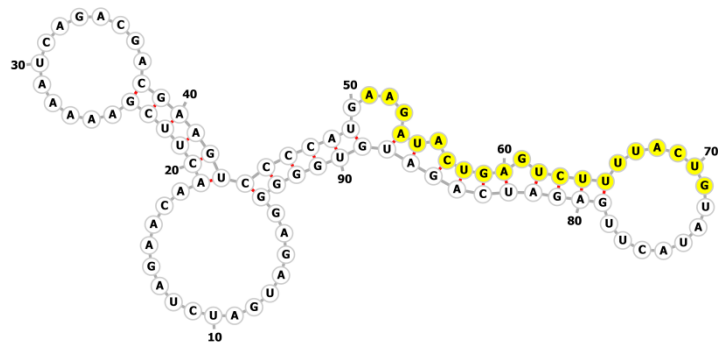
37



45



52

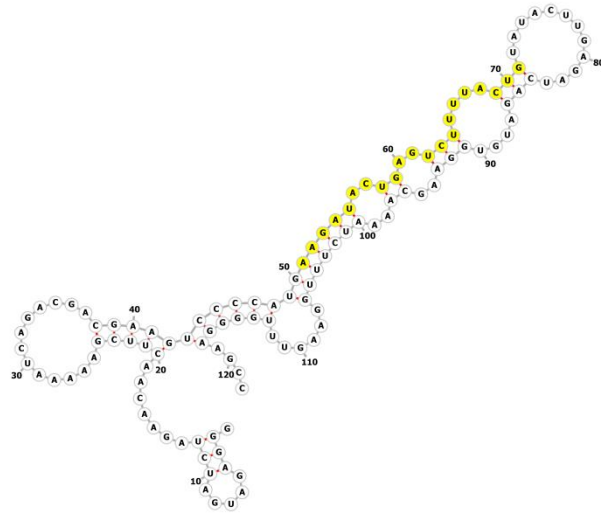


lin-122

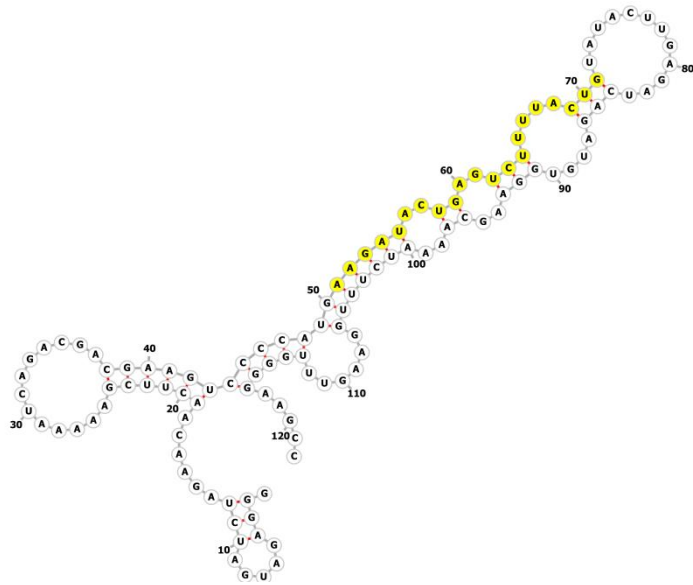
GGGAGAUGAUCUAGAACAACUUCGAAAAAUCAGACGACGAAGUCCCAUGAAGAUACU
 GAGUCUUUUACUGUAUACUUGAGAUCAGAUGUGGAAGCAAUAUCUUUGGAAGUUUGG
 GGAAGCC

Temperature [°C]	Secondary structure
13	
20	

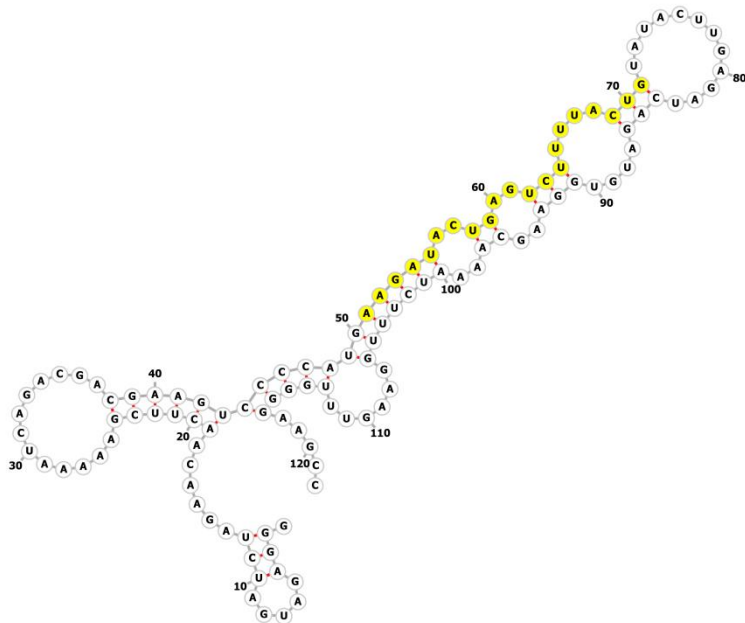
25
(continued lin-122)



30

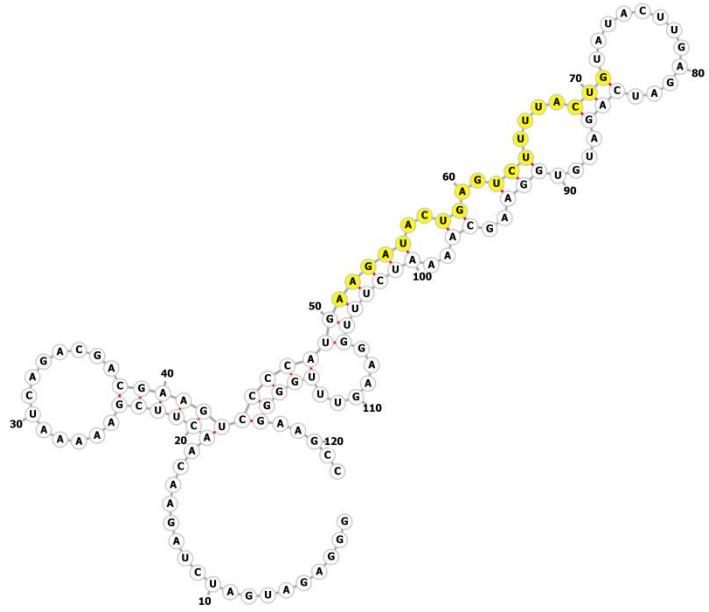


37

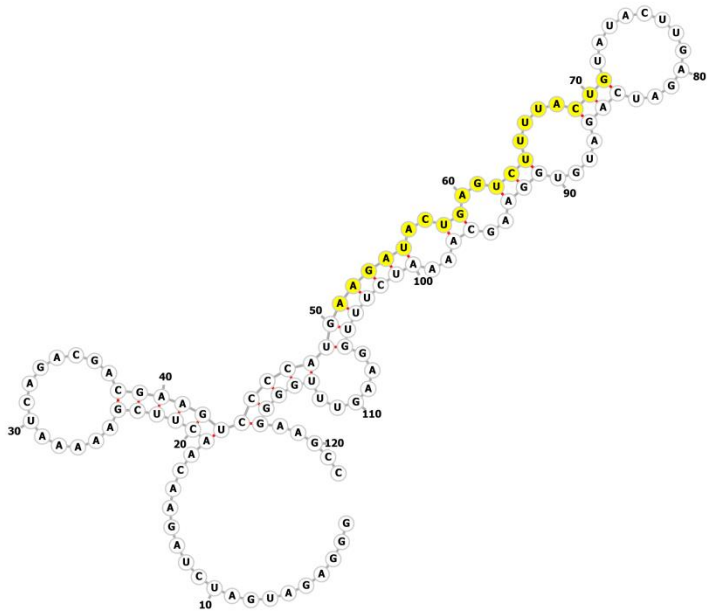


(continued lin-122)

45



52



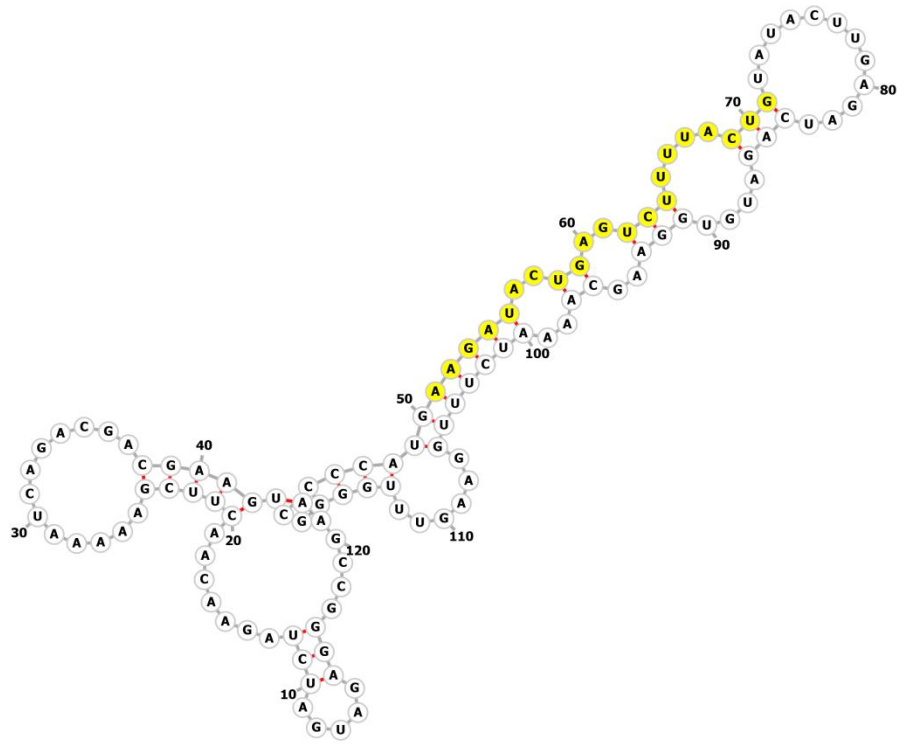
circ-122

GGGAGAUGAUCUAGAACAACUUCGAAAAUCAGACGACGAAGUCCCCAUGAAGAUACU
 GAGUCUUUUACUGUAUACUUGAGAUCAGAUGUGGAAGCAAUAUCUUUGGAAGUUUGG
 GGAAGCC

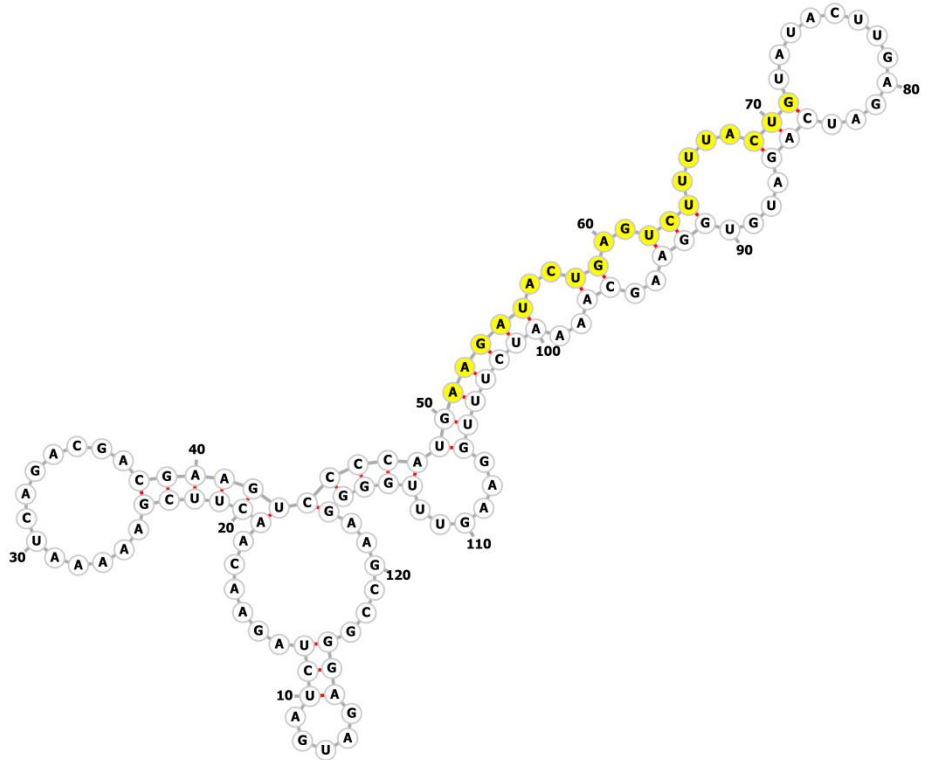
Temperature [°C]	Secondary structure
13	
20	

(continued
circ-122)

25

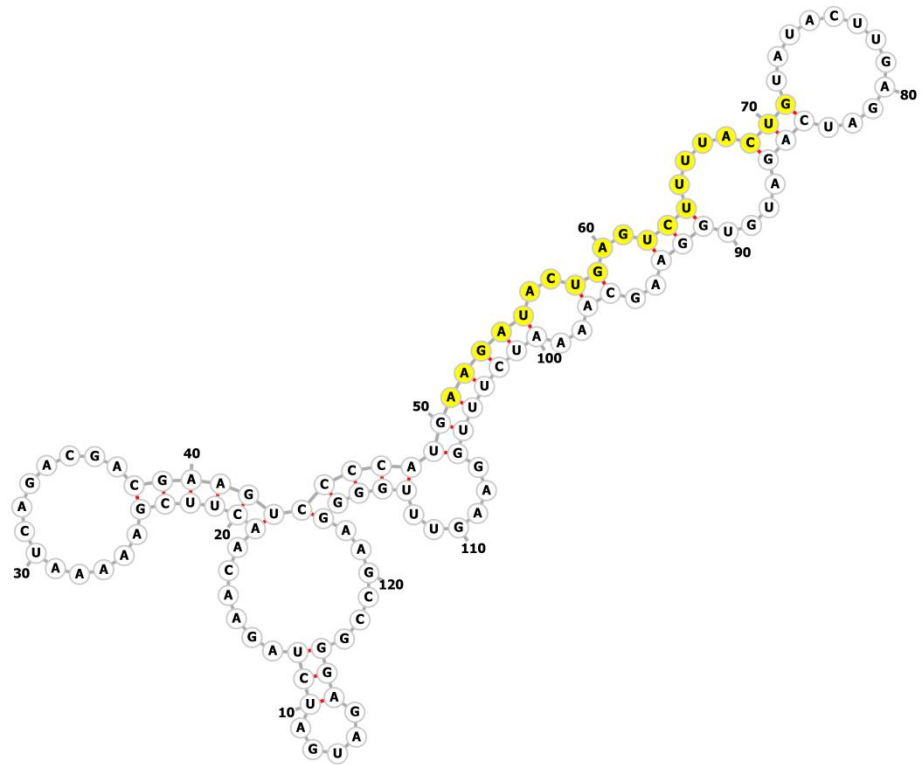


30

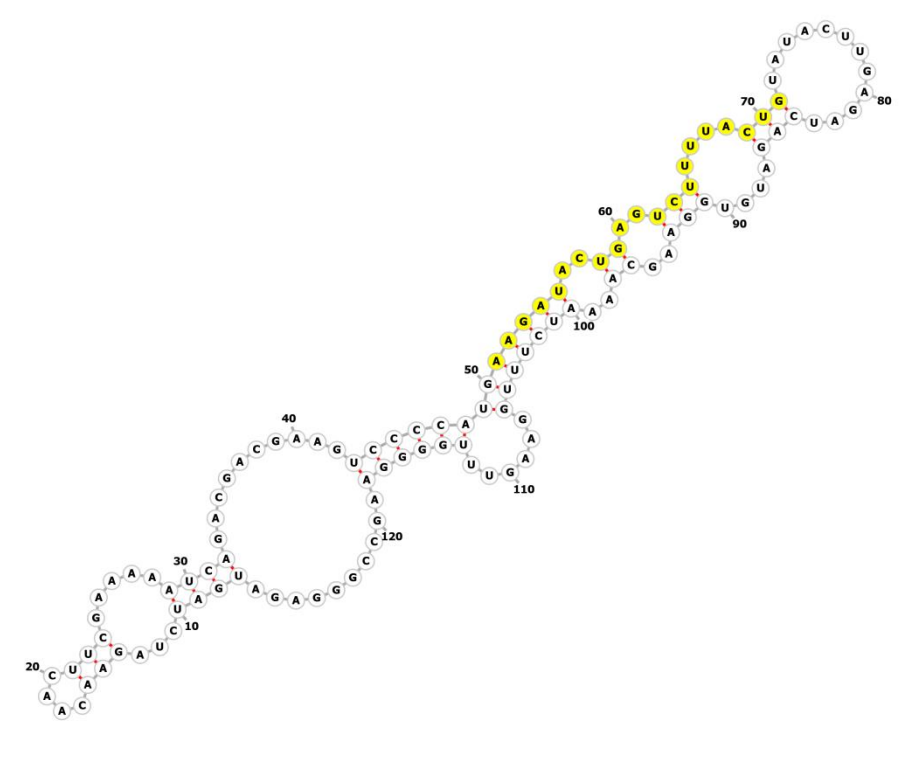


(continued
circ-122)

37

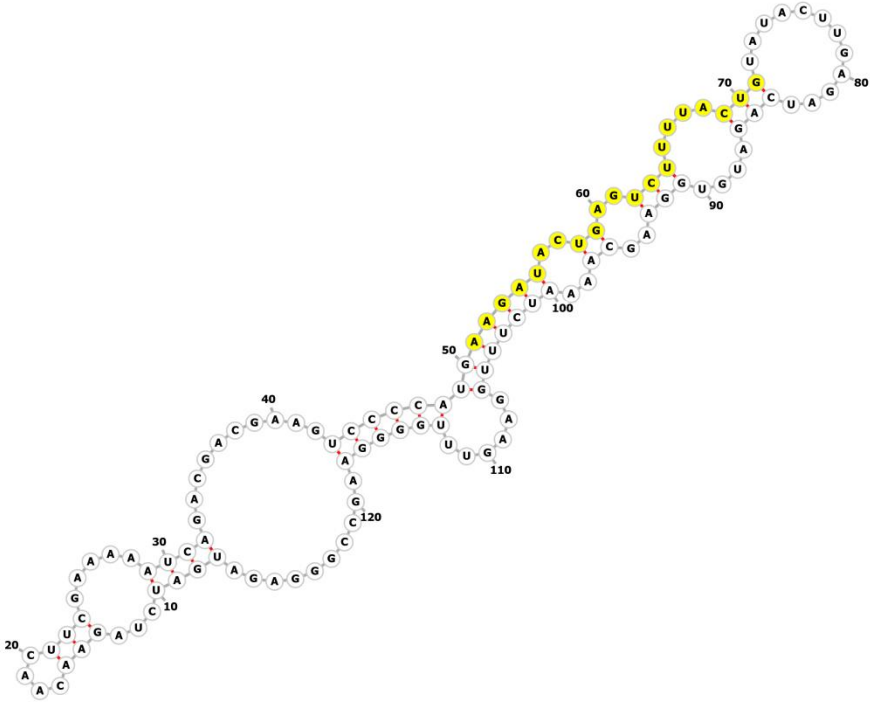


45



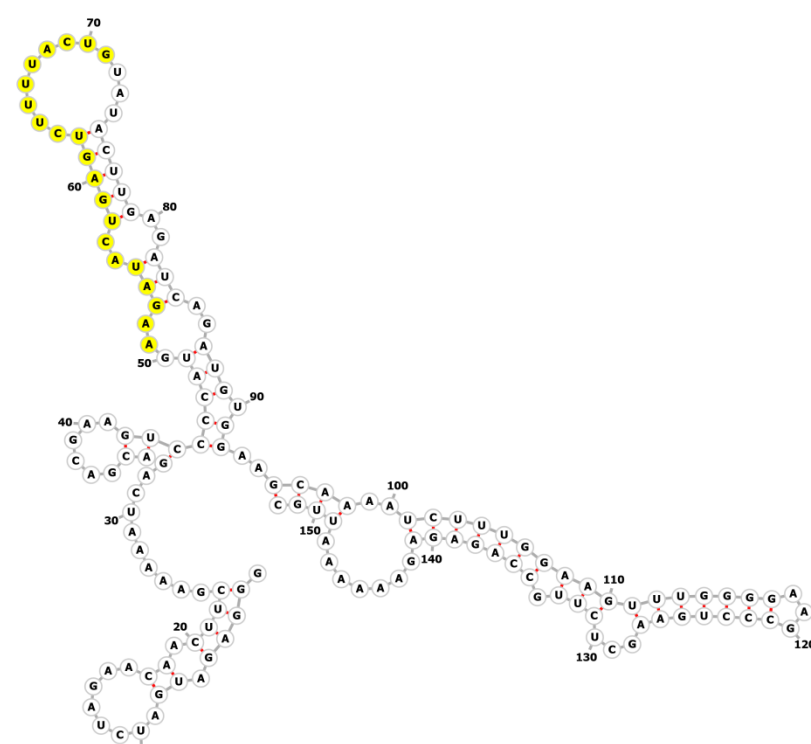
(continued
circ-122)

52



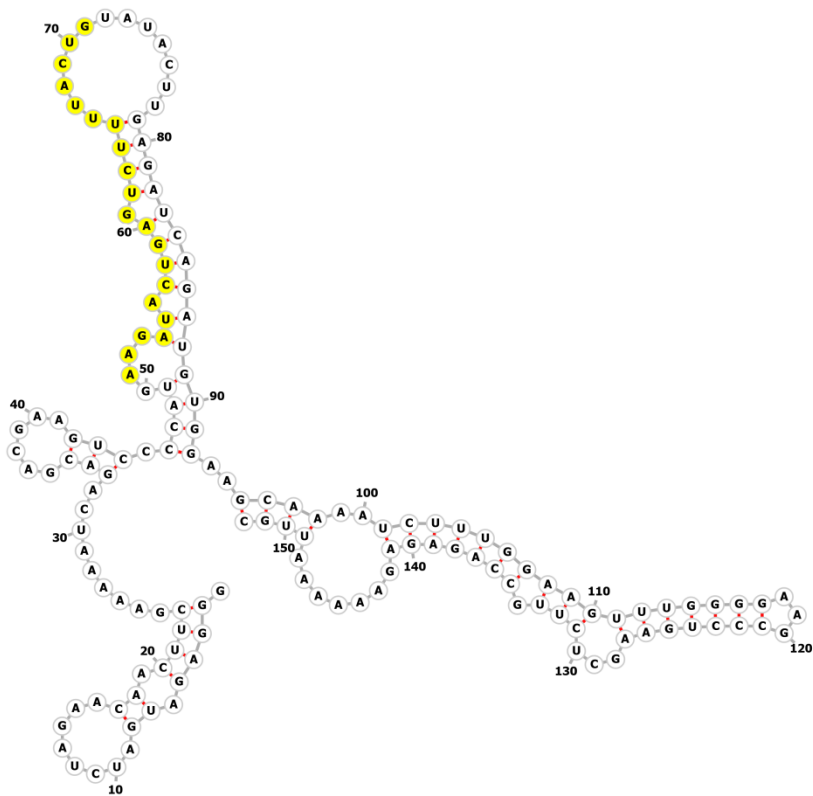
lin-152

GGGAGAUGAUCUAGAACAACUUCGAAAAAUCAGACGACGAAGUCCCAUGAAGAUACU
GAGUCUUUUACUGUAUACUUGAGAUCAGAUGUGGAAGCAAAAUCUUUGGAAGUUUGG
GGAAGCCCUGAAGCUCUUGCCAGAGAGAAAAAUUGC

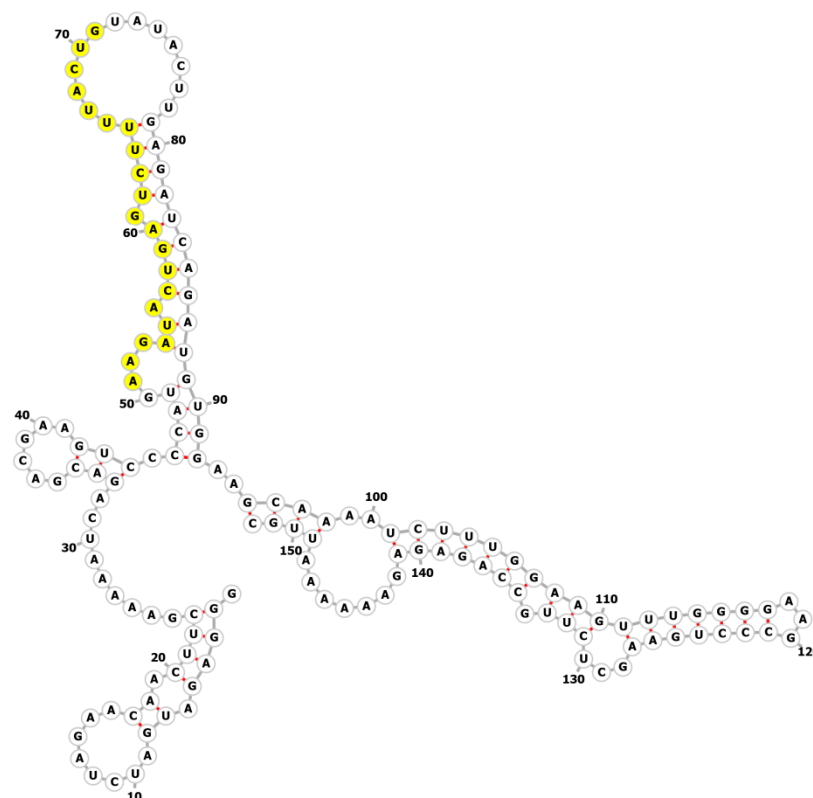
Temperature [°C]	Secondary structure
13	

(continued
lin- 152)

20

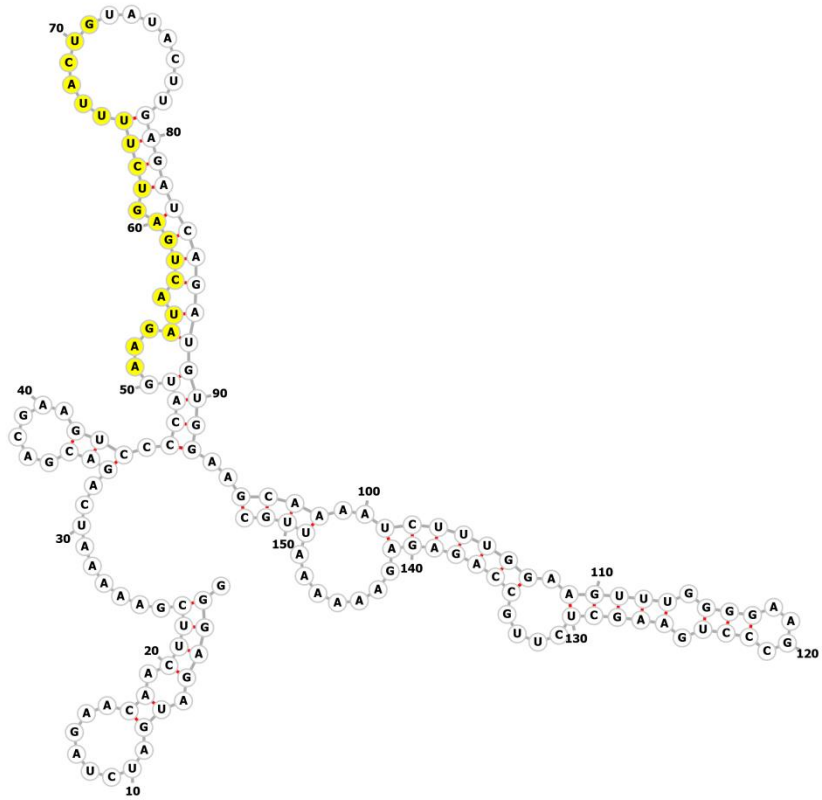


25

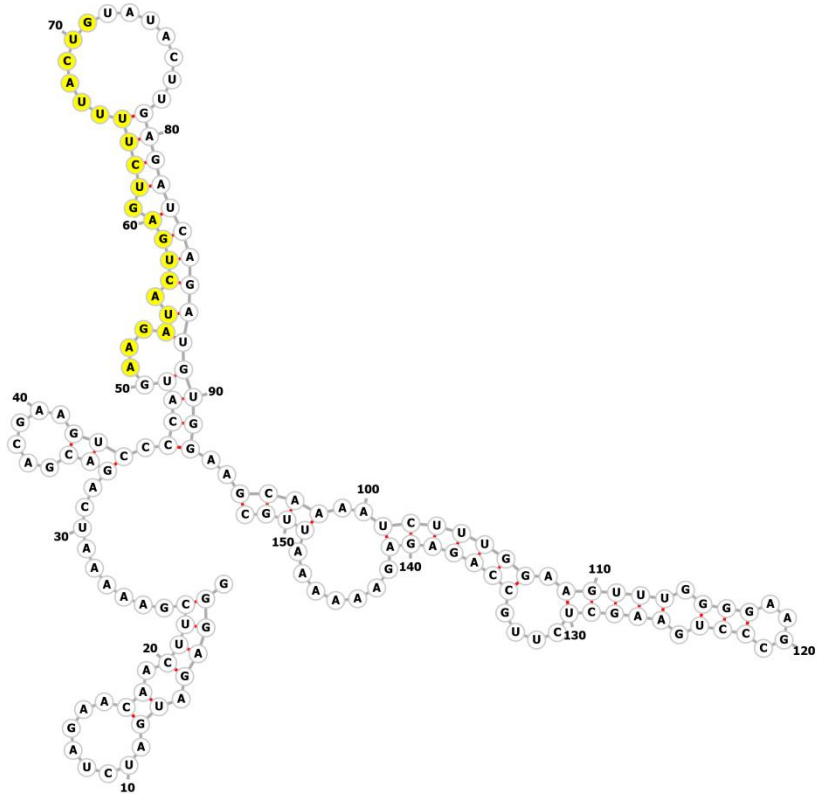


(continued
lin-152)

30

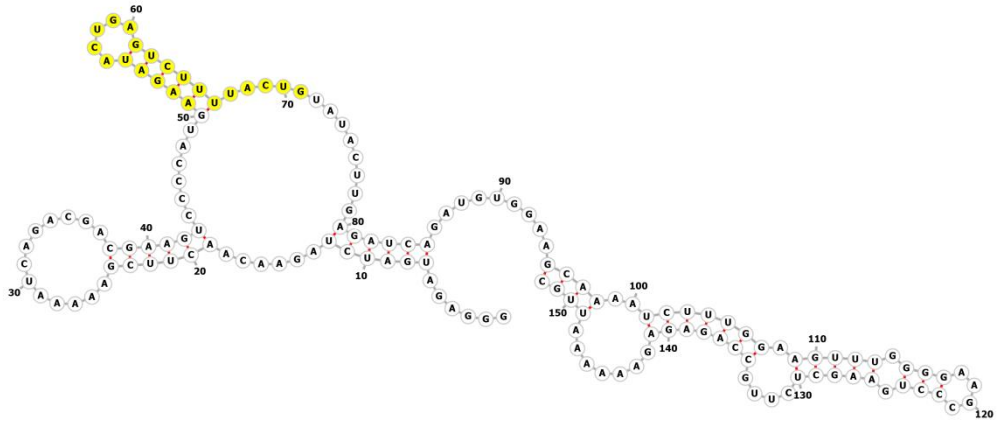


37

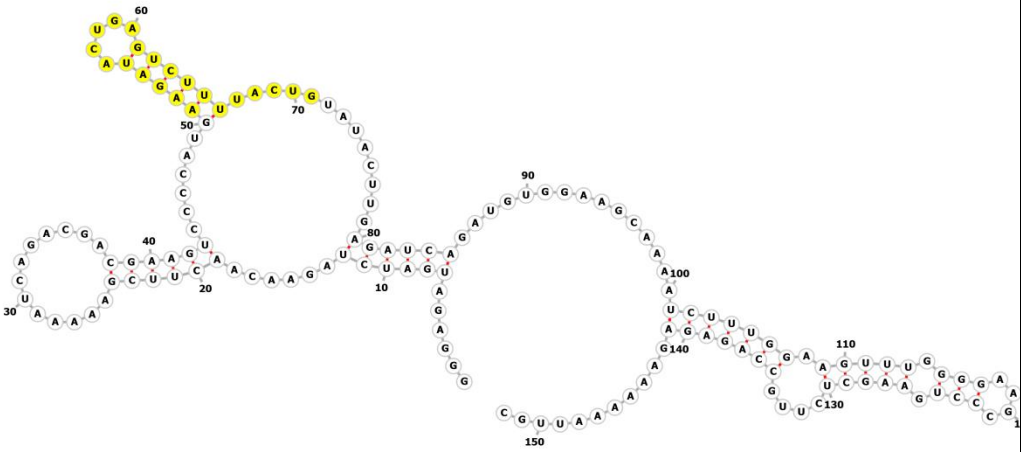


(continued
lin-152)

45

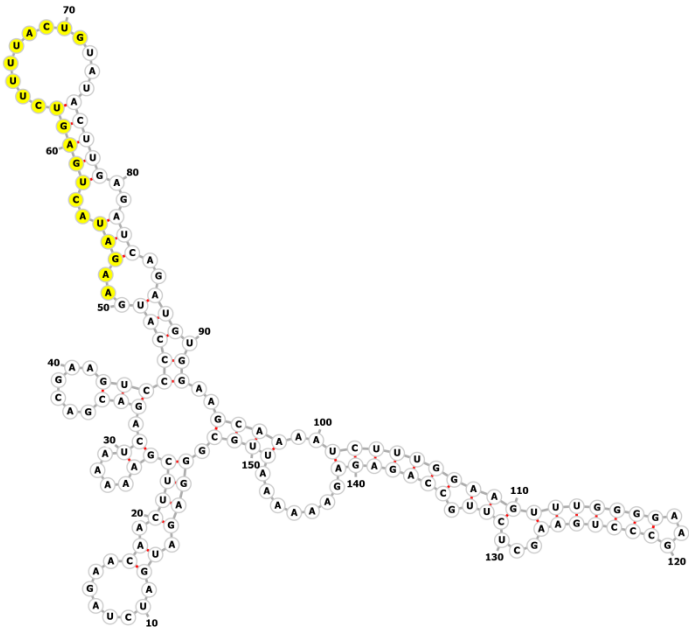
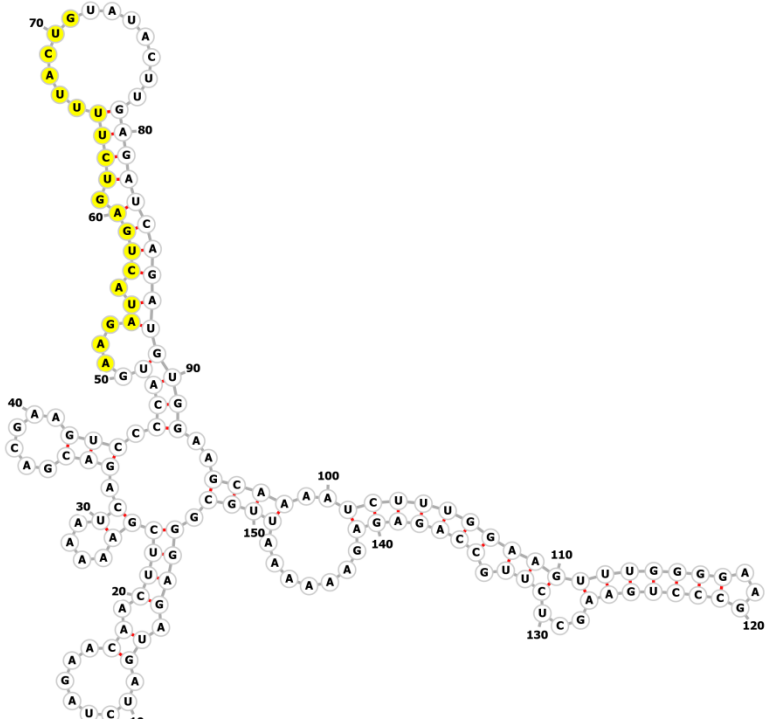


52



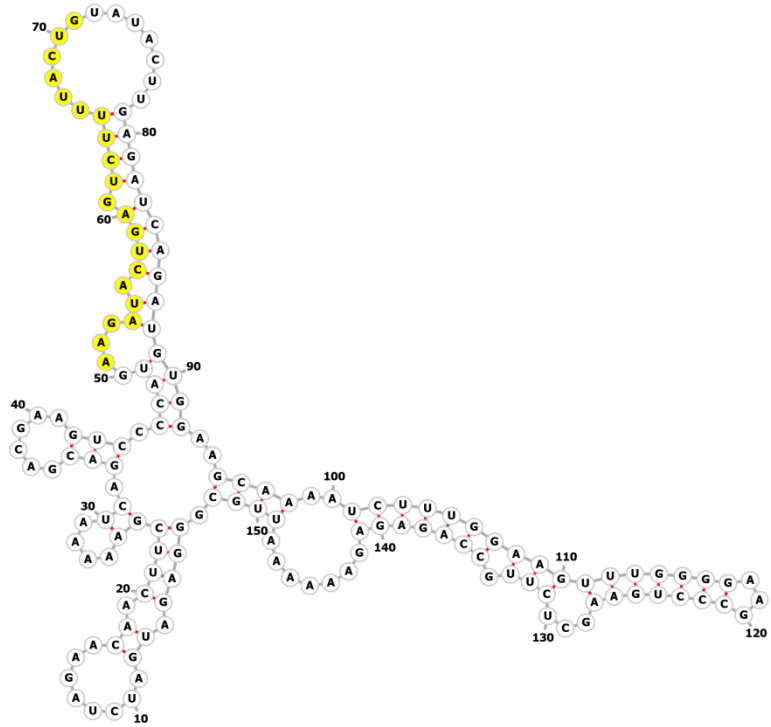
circ-152

GGGAGAUGAUCUAGAACAACUUCGAAAAAUCAGACGACGAAGUCCCAUGAAGAUACU
 GAGUCUUUUACUGUAUACUUGAGAUCAGAUGUGGAAGCAAAAUCUUUGGAAGUUUGG
 GGAAGCCCUGAAGCUCUUGCCAGAGAGAAAAAUUGC

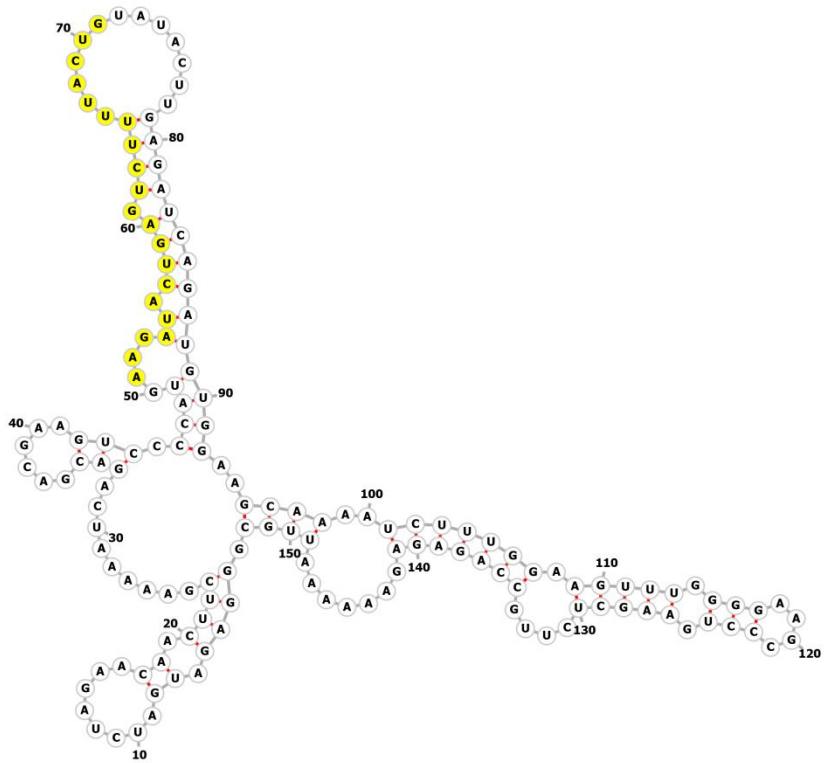
Temperature [°C]	Secondary structure
13	
20	

(continued
circ-152)

25

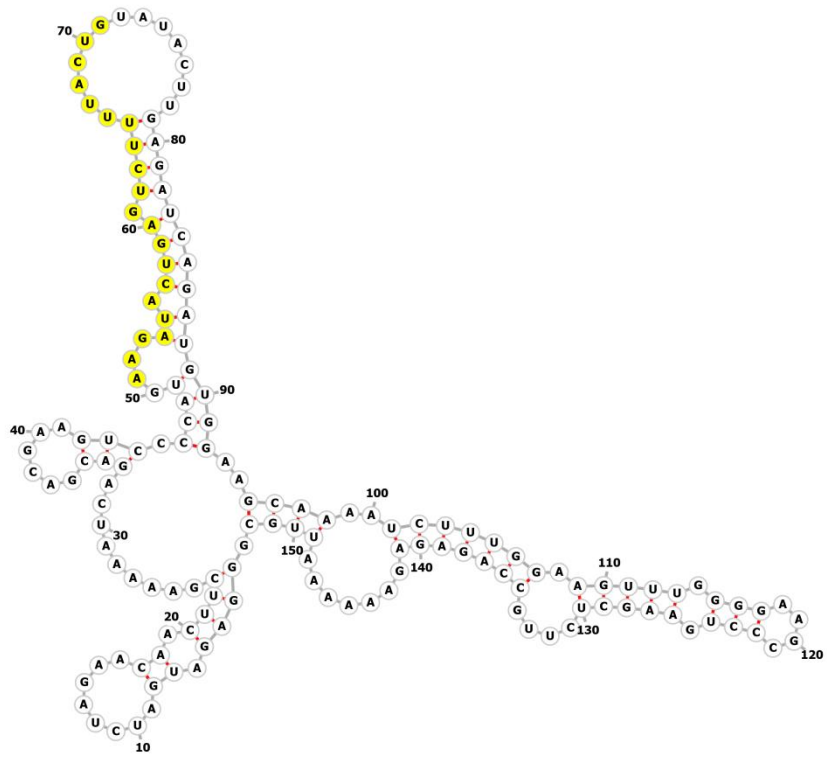


30

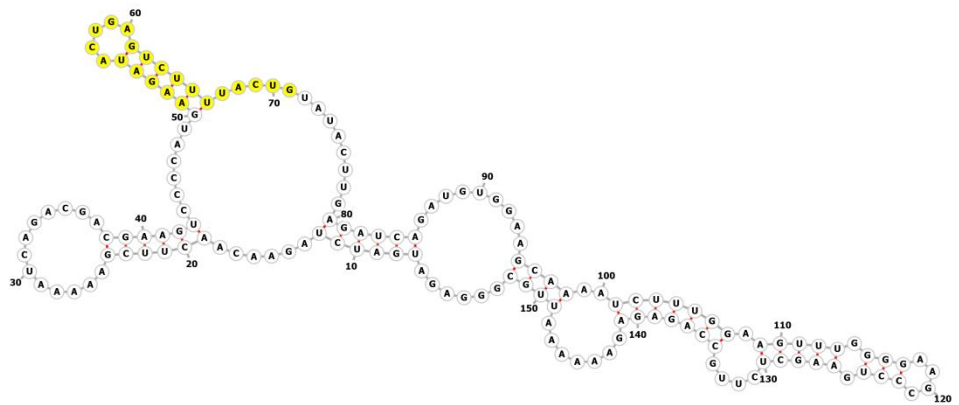


(continued
circ-152)

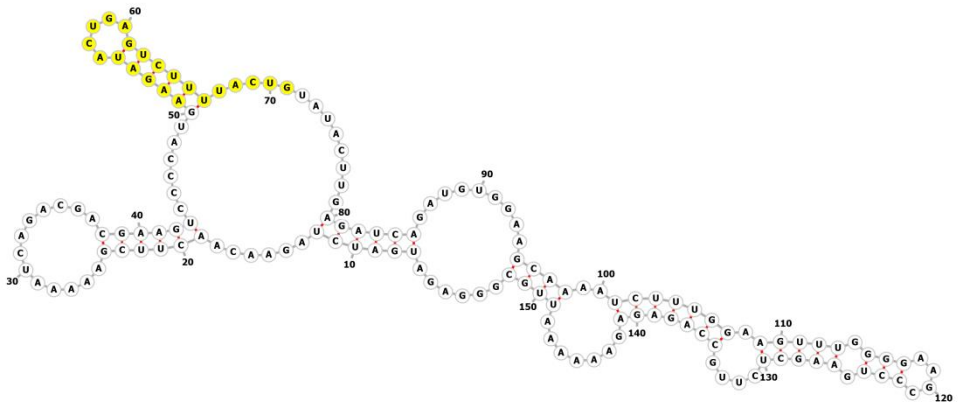
37



45



52



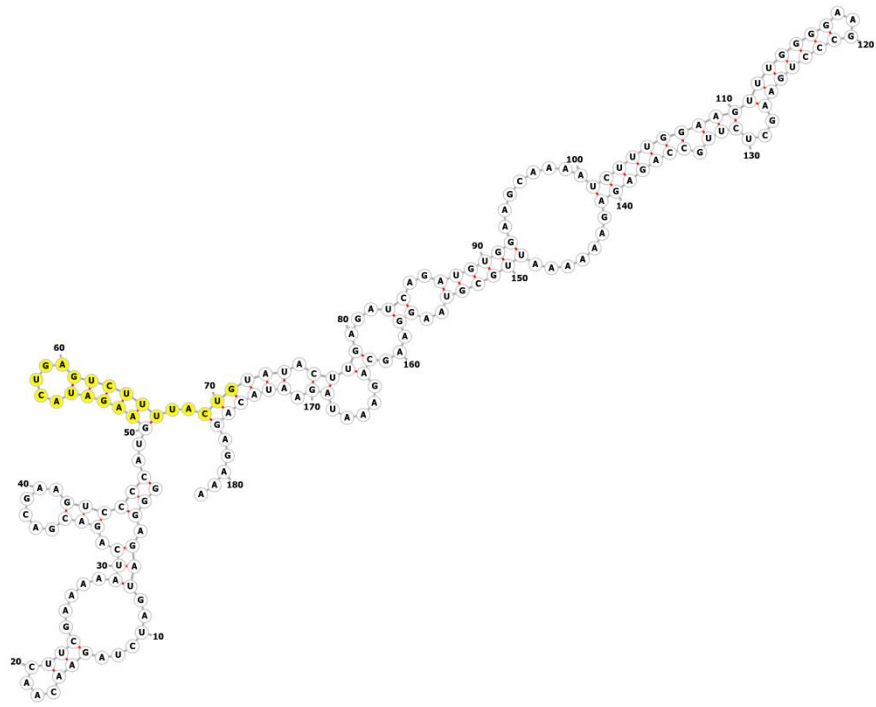
lin-182

GGGAGAUGAUCUAGAACAACUUCGAAAAAUCAGACGACGAAGUCCCAUGAAGAUACU
 GAGUCUUUUACUGUAUACUUGAGAUCAGAUGUGGAAGCAAAAUCUUUGGAAGUUUGG
 GGAAGCCCUGAAGCUCUUGCCAGAGAGAAAAAUUGCGUAAGGAAGCAGAAUAGAAU
 ACAGAGAAA

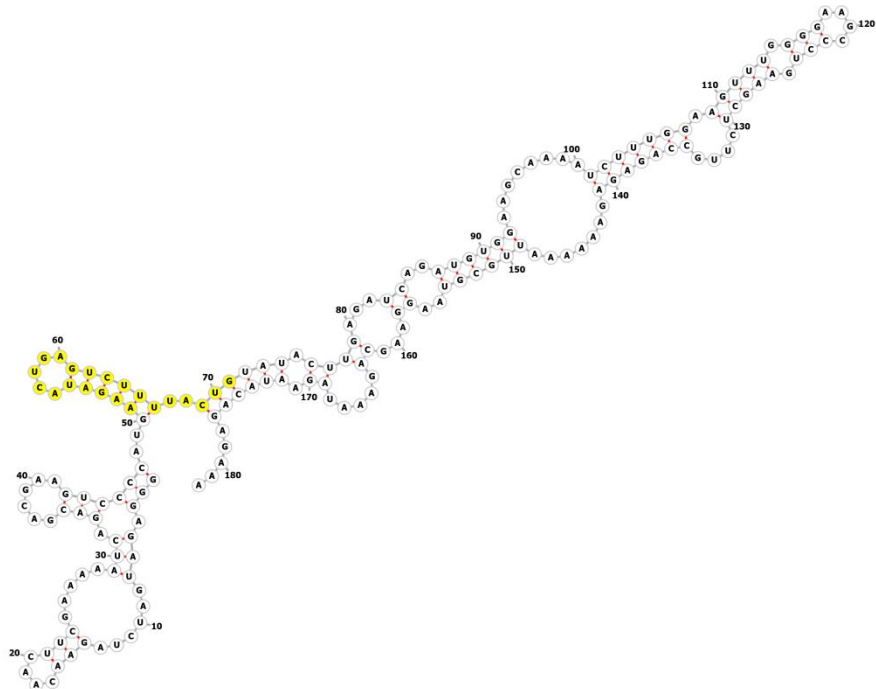
Temperature [°C]	Secondary structure
13	
20	

(continued
lin-182)

25

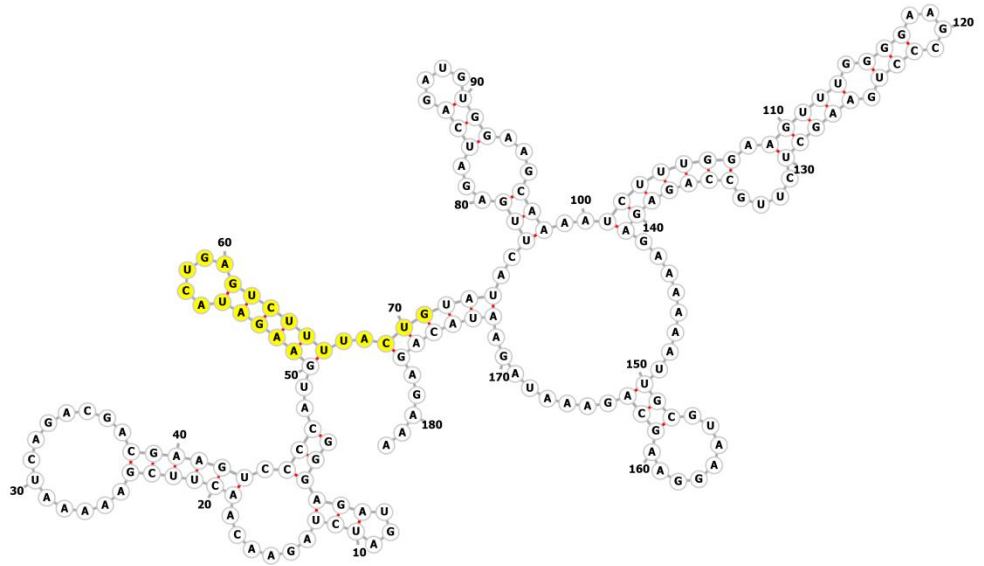


30

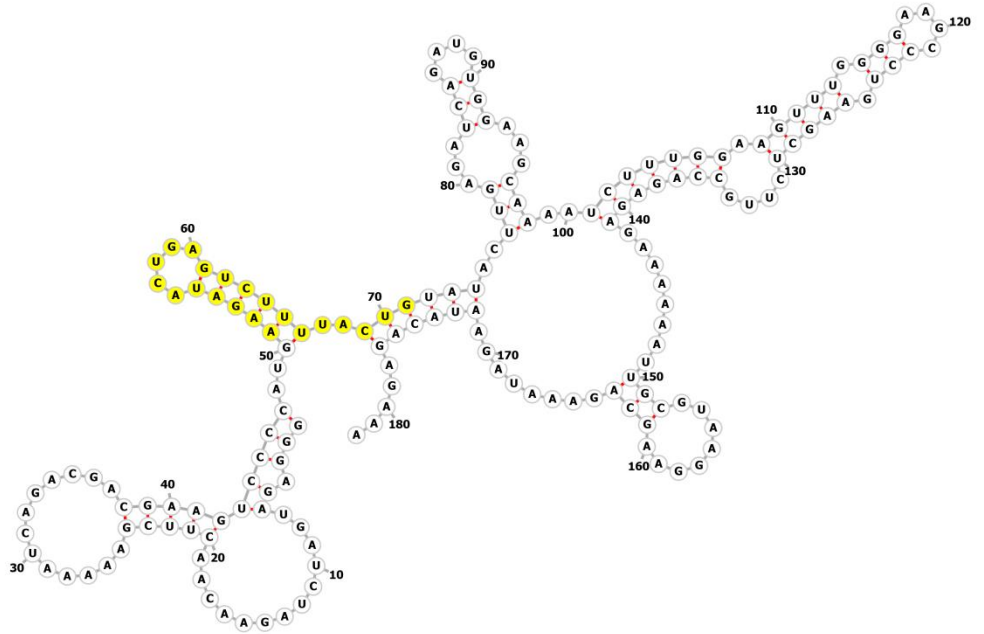


(continued
lin-182)

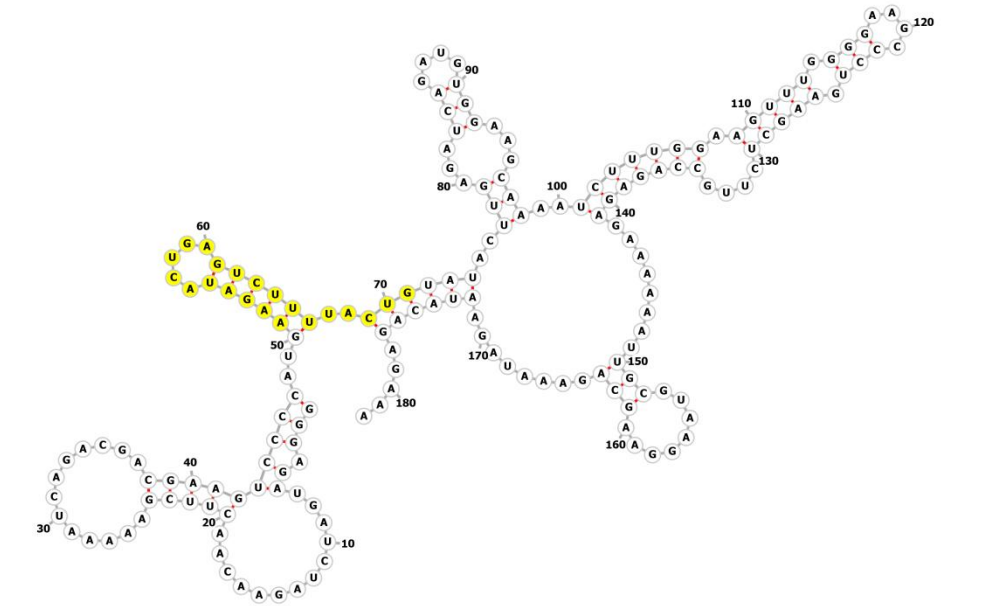
37



45

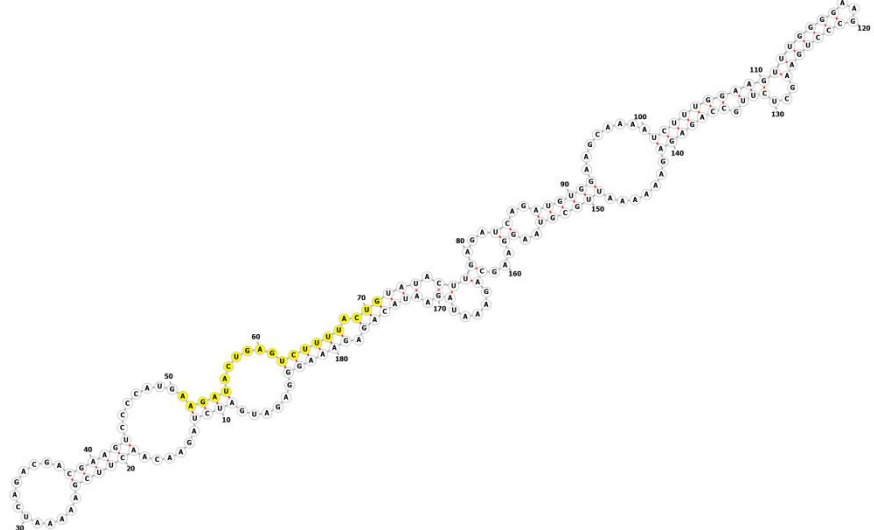
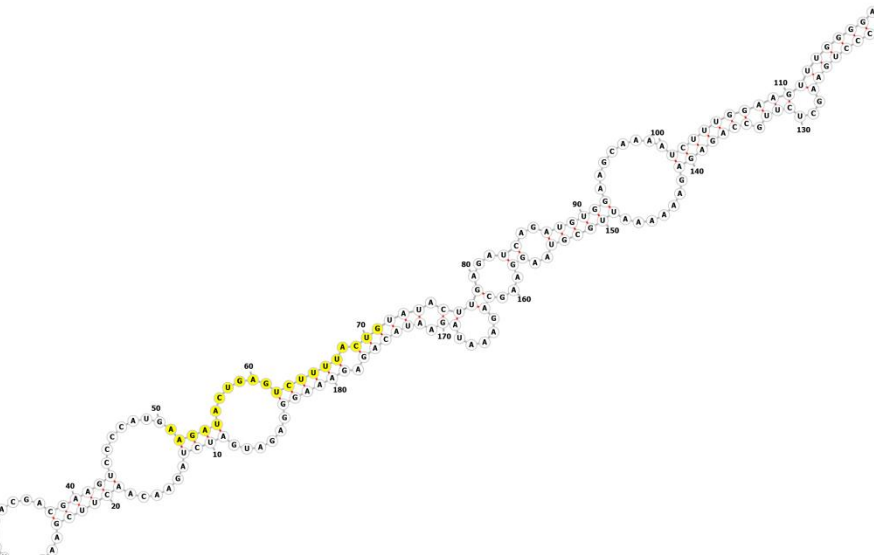


52



circ-182

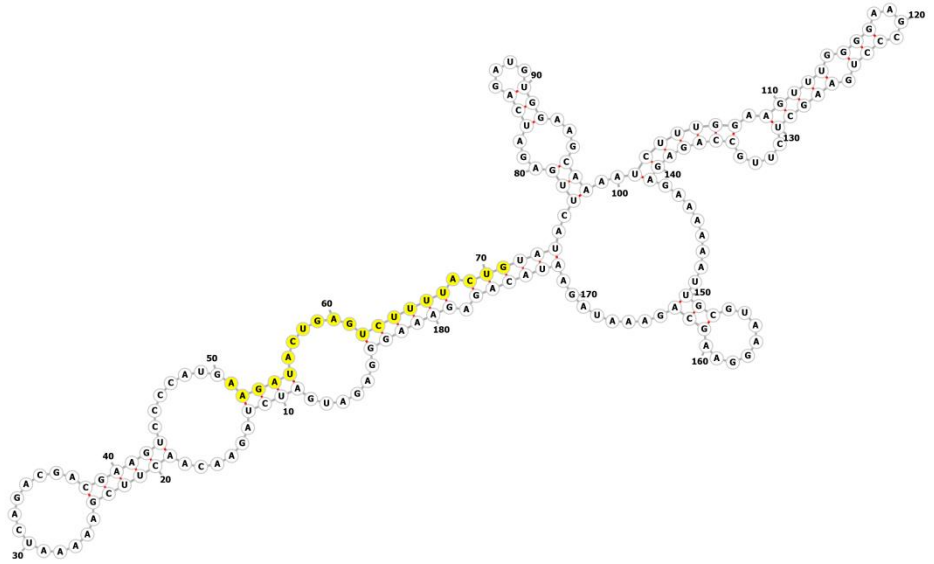
GGGAGAUGAUCUAGAACAACUUCGAAAAAUCAGACGACGAAGUCCCAUGAAGAUACU
 GAGUCUUUUACUGUAUACUUGAGAUCAGAUGUGGAAGCAAAAUCUUUGGAAGUUUGG
 GGAAGCCCUGAAGCUCUUGCCAGAGAGAAAAAUUGCGUAAGGAAGCAGAAUAGAAU
 ACAGAGAAA

Temperature [°C]	Secondary structure
13	
20	

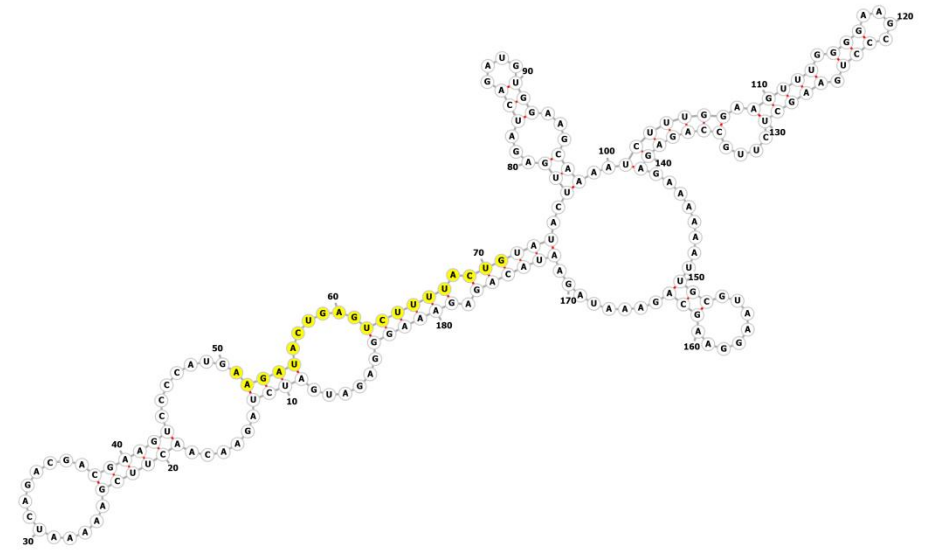
<p>(continued circ-182)</p> <p>25</p>	
<p>30</p>	
<p>37</p>	

(continued
circ-182)

45



52



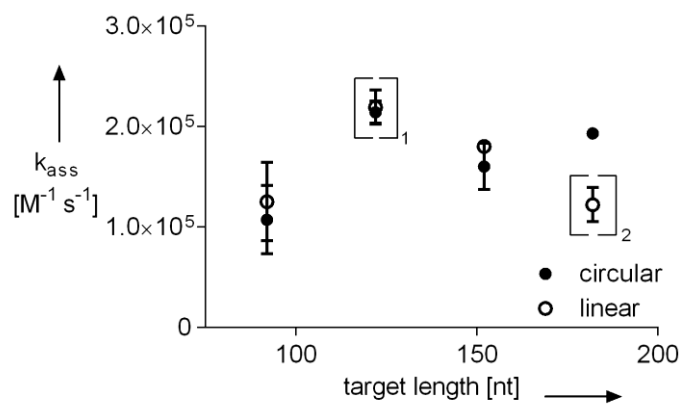


Figure S2 Dependency of rate constants on RNA length and topology. All kinetic measurements were performed at 37 °C and time points of 0, 1, 2, 4, 8, and 16 min, respectively. Footnotes see Table S4.

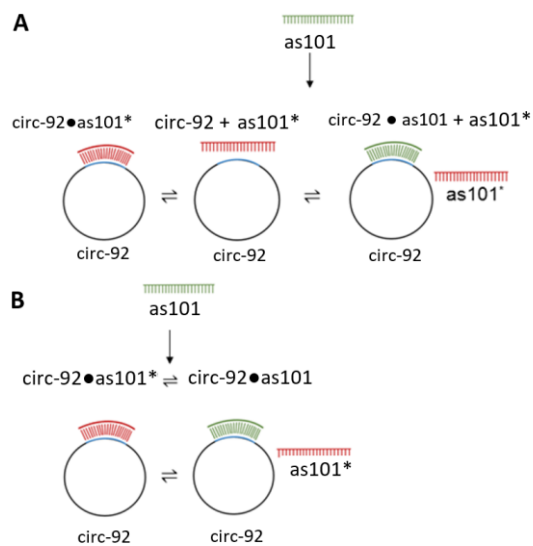


Figure S3 Associative pathway vs. dissociative pathway in the sequence system of this work. Two possible mechanisms for the dissociation of circ-RNA-bound oligoribonucleotides have to be considered. **(A)** Dissociative mechanism, the complex composed of circ-92 and as101* dissociates and produces two single-strands. Free unlabeled as101 binds to the free circ-92. **(B)** Associative mechanism, the complex of circ-92 and as101* encounters a free unlabeled as101 (green) and forms a ternary complex which leads to the displacement of as101* (red) and formation of a new complex consisting of circ-92 and as101.

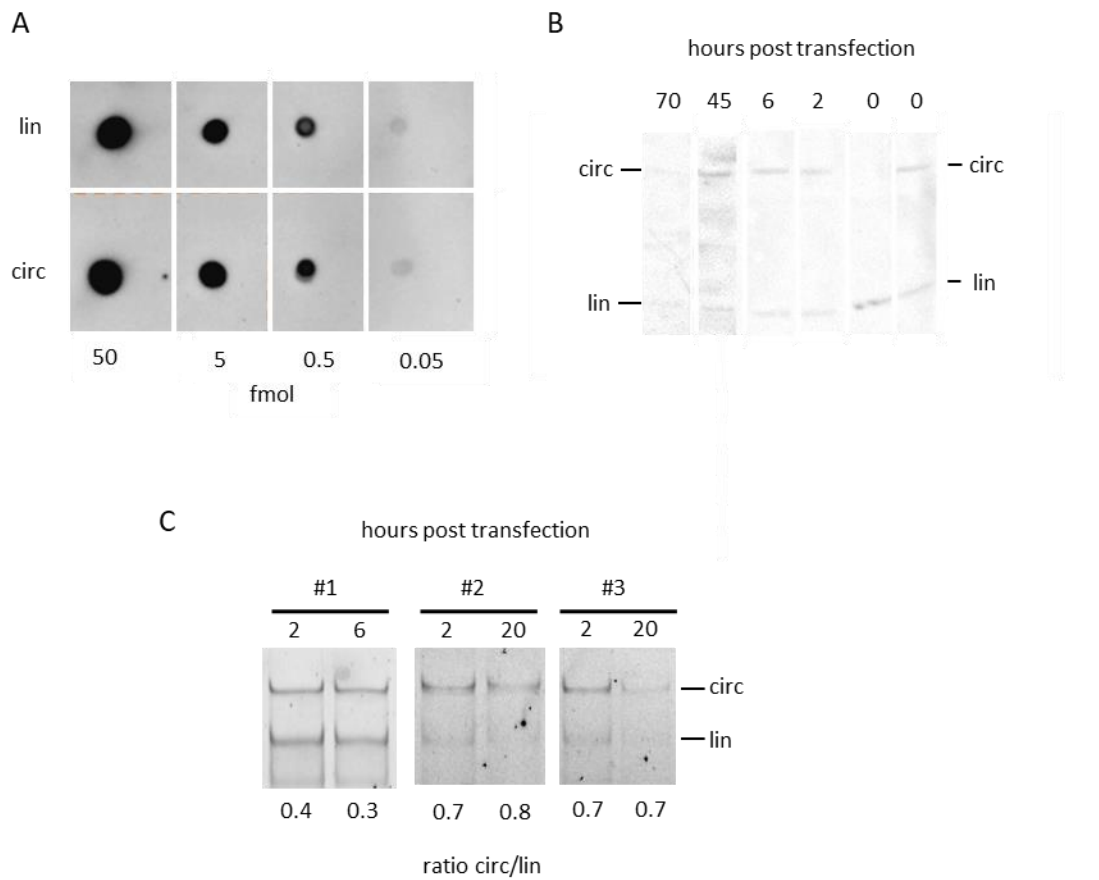


Figure S4 Intracellular amounts of lin-92 and circ-92, respectively after transfection. (A) Dot blots of a dilution series of lin-92 and circ-92 probed with FAM-labeled probe. **(B)** Northern analysis of total RNA prepared from transfected cells at various time points after transfection (indicated on top). At time point '0' a mixture of lin-92/circ-92 was separated (right panel) while lin-92 is shown on the 2nd lane from the right. Please note that lanes were cut out of different gels and put together in this panel. **(C)** Liquid hybridization assay. Total cellular RNA was incubated with a FAM-labeled completely matching probe (5'-FAM-as101) and complexes visualized by polyacrylamide gel electrophoresis. Quantification of signals was performed by the ImageQuant software package. The time points after transfection of three individual experiments are shown (#1 - #3) and the ratio of signals of linear and circular RNAs are indicated below.

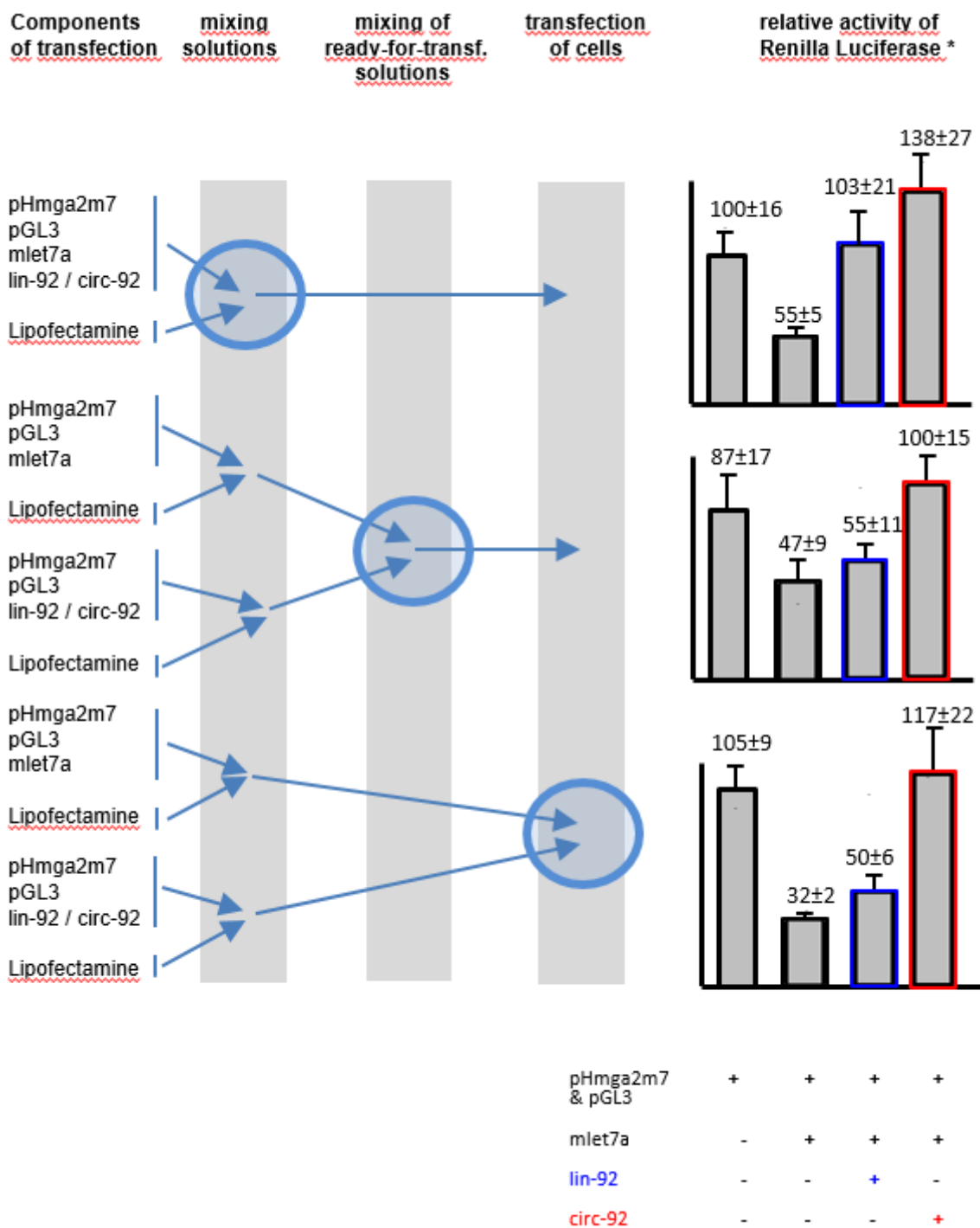


Figure S5 The order of the transfection of plasmids and RNAs does not influence the observations of competing lin-92/circ-92. Scheme showing different orders of adding components of the transfection assay (Figure 3C & D) aiming to study the level of RNA-RNA interactions between mlet7a and forms of mlet7a-92. The left side shows components of transfection and the order of mixing. Circles in blue indicate the step at which mlet7a and mlet7a-92 RNAs encounter for the first time. The right panel shows experimental results for competing effects by lin-mlet7a-92 and by circ-mlet7a-92, respectively. The Y-axis indicates relative luciferase expression normalized in the dual luciferase assay..

Table S1 Full length RNA sequences (182-92mer)

182mer (hsa_circ_000391 is obtained by replacing the starting hexanucleotide "GGG AGA", introduced due to the synthesis strategy.)	5'-GGG AGA UGA UCU AGA ACA ACU UCG AAA AAU CAG ACG ACG AAG UCC CCA UGA AGA UAC UGA GUC UUU UAC UGU AUA CUU GAG AUC AGA UGU GGA AGC AAA AUC UUU GGA AGU UUG GGG AAG CCC UGA AGC UCU UGC CAG AGA GAA AAA AUU GCG UAA GGA AGC AGA AAU AGA AUA CAG AGA AA-3'
152mer	5'-GGG AGA UGA UCU AGA ACA ACU UCG AAA AAU CAG ACG ACG AAG UCC CCA UGA AGA UAC UGA GUC UUU UAC UGU AUA CUU GAG AUC AGA UGU GGA GCA AAA UCU UUG GAA GUU UGG GGA AGC CCU GAA GCU CUU GCC AGA GAG AAA AAA UUG C-3'
122mer	5'-GGG AGA UGA UCU AGA ACA ACU UCG AAA AAU CAG ACG ACG AAG UCC CCA UGA AGA UAC UGA GUC UUU UAC UGU AUA CUU GAG AUC AGA UGU GGA AGC AAA AUC UUU GGA AGU UUG GGG AAG CC-3'
92mer	5'-GGG AGA UGA UCU AGA ACA ACU UCG AAA AAU CAG ACG ACG AAG UCC CCA UGA AGA UAC UGA GUC UUU UAC UGU AUA CUU GAG AUC AGA UGU GG-3'
lin-/circ-mlet7a-92	5'-GGG AGA UGA UCU AGA ACA AAC UAU ACA ACC UAC UAA CGC AAG UCC CAA GAU ACU GAG UCU UCA UUA CUG UAU ACU UGU GAG AUC AGA UGU CU-3'

Table S2 Sequences of small antisense RNAs and miRNAs.

as101	5'-AUA CAG UAA AAG ACU CAG UAU-3'
ds mlet7A antisense	5'-UGC GUU AGU AGG UUG UAU AGU UU-3'
ds mlet7A sense	5'-ACU AUA CAA UCU ACU GGC GUU CC-3'
as scramble RNA	5'-GGU CAG ACC AGU CAG UUC GTT -3'
si-scr	5'-CGA ACU CAC UGG UCU GAC CTT -3'

* At the 5' or 3' position a 6-FAM- label were introduced. Rate constants revealed no influence of the label position. Additionally, using a 5'-³²P instead of a FAM-label, did not show any differences regarding the rate constants.

** Protruding ends are marked in bold.

Table S3 Klenow primer sequences for generation of double-stranded DNA templates for *in vitro* transcription and sequence of stocking oligonucleotide

circ1406_182_fw	5'-TAA TAC GAC TCA CTA TAG <u>GGA GAT GAT</u> CTA GAA CAA CTT CGA AAA ATC AGA CGA CGA AGT CCC CAT GAA GAT ACT GAG TCT TTT ACT GTA TAC TTG AGA TCA GAT GTG GAA-3'
circRNA1406_182_rv	5'-TTT CTC TGT ATT CTA TTT CTG CTT CCT TAC GCA ATT TTT TCT CTC TGG CAA GAG CTT CAG GGC TTC CCC AAA CTT CCA AAG ATT TTG CTT CCA CAT CTG ATC TCA AGT AT-3'
circRNA_1406_152_fw	5'-TAA TAC GAC TCA CTA TAG <u>GGA GAT GAT</u> CTA GAA CAA CTT CGA AAA ATC AGA CGA CGA AGT CCC CAT GAA GAT ACT GAG TCT TTT ACT GTA TAC TT-3'
circRNA_1406_152_rv	5'-GCA ATT TTT TCT CTC TGG CAA GAG CTT CAG GGC TTC CCC AAA CTT CCA AAG ATT TTG CTT CCA CAT CTG ATC TCA AGT ATA CAG TAA AAG ACT CA-3'
circRNA_1406_122_fw (identical to circRNA_1406_152_fw)	5'-TAA TAC GAC TCA CTA TAG <u>GGA GAT GAT</u> CTA GAA CAA CTT CGA AAA ATC AGA CGA CGA AGT CCC CAT GAA GAT ACT GAG TCT TTT ACT GTA TAC TT-3'
circRNA_1406_122_rv	5'-GGC TTC CCC AAA CTT CCA AAG ATT TTG CTT CCA CAT CTG ATC TCA AGT ATA CAG TAA AAG ACT CAG-3'
circRNA_1406_92_fw	5'-TAA TAC GAC TCA CTA TAG <u>GGA GAT GAT</u> CTA GAA CAA CTT CGA AAA ATC AGA CGA CGA AGT CCC C-3'
circRNA_1406_92_rv	5'-CCA CAT CTG ATC TCA AGT ATA CAG TAA AAG ACT CAG TAT CTT CAT GGG GAC TTC GTC TC-3'
92R_comp_fwd (for the reservoir used in BCa cells)	5'-TAA TAC GAC TCA CTA TAG <u>GGA GAT GAT</u> CTA GAA CAA ACT ATA CAA CCT ACT AAC GCA AGT CCC-3'
92R_comp_rev (for the reservoir used in BCa cells)	5'-AGA CAT CTG ATC TCA CAA GTA TAC AGT AAT GAA GAC TCA GTA TCT TGG GAC TTG CGT TAG TAG GTT GTA TAG-3'

Underlined sequences display one strand of the T7 RNA polymerase promoter sequence

Table S4 Dependency of rate constants on RNA length and topology

Topology	length [nt]	k_{ass} im $\text{M}^{-1} \text{s}^{-1}$
linear	92	$1.25 \cdot 10^5 \pm 0.39 \cdot 10^5$
circular		$1.07 \cdot 10^5 \pm 0.34 \cdot 10^5$
linear	122 ₁	$2.19 \cdot 10^5 \pm 0.17 \cdot 10^5$
circular		$2.19 \cdot 10^5 \pm 0.11 \cdot 10^5$
linear	152	$1.86 \cdot 10^5 \pm 1.40 \cdot 10^5$
circular		$1.60 \cdot 10^5 \pm 0.23 \cdot 10^5$
linear	182 ₂	$1.22 \cdot 10^5 \pm 0.23 \cdot 10^5$
circular		$1.93 \cdot 10^5 \pm 0.04 \cdot 10^5$

¹ According to predicted secondary structure, the 122mers display as101 binding sites at 37 °C that differs from those of the other RNAs used in this assay at 37 °C.

² Interpretation of linear 182mers data was challenging due to quenching effects and additional products bands indicating lower molecular weight, most probably caused by beginning RNA degradation. This may lead to RNAs with unknown structures/accessibilities of as101 binding sites as well as changes of the concentration of lin-182.

Table S5 Thermodynamic parameter of the association of as101 to the 92mers, lin-92 and circ-92.

temperature [°C]	[K]	ΔG^\ddagger [kJ/mol]		ΔH^\ddagger [kJ/mol]		$T\Delta S^\ddagger$ [kcal/mol]		$T\Delta S^\ddagger$ [eu]	
		linear	circular	linear	circular	linear	circular	linear	circular
13	286.15	44.2	47.2	30.1	55.2	-3354.7	1920.6	-11.7	6.7
20	293.15	44.6	45.5	30.1	55.2	-3461.5	2321.6	-11.8	7.9
25	298.15	45.2	47.4	30.0	55.1	-3617.7	1857.6	-12.1	6.2
30	303.15	46.4	47.2	30.0	55.1	-3925.0	1895.2	-12.9	6.3
37	310.15	45.8	46.2	29.9	55.0	-3792.7	2114.2	-12.2	6.8
45	318.15	45.7	44.9	29.9	55.0	-3783.1	2398.5	-11.9	7.5
52	325.15	46.3	46.4	29.8	54.9	-3934.7	2039.9	-12.1	6.3